Chemical and biological sensors

# A Wearable and Multiplexed Electrochemical Sensor Suite for Real-Time Sweat Ionic Content and pH Monitoring With IoT Integration

Nafize Ishtiaque Hossain[1,2], Atul Sharma[1,2], and Sameer Sonkusale[1,2]

[1]*Nano Lab, Advanced Technology Laboratory, Tufts University School of Engineering, Medford, MA 02155 USA*
[2]*Department of Electrical and Computer Engineering, Tufts University School of Engineering, Medford, MA 02155 USA*

Manuscript received 18 July 2023; accepted 20 July 2023. Date of publication 1 August 2023; date of current version 14 August 2023.

Abstract—Noninvasive sweat sensor integrated with electronic devices has great potential to monitor health conditions and diagnose several diseases in their early stages. In this letter, we present multiplexed flexible skin patches consisting of electrochemical sensors for monitoring potassium ($K^+$), calcium ($Ca^{2+}$), and pH levels in sweat with Internet-of-Things (IoT) connectivity. The sensor suite demonstrates dynamic and repeatable characteristics with a high degree of sensitivity ($S_K^+ = 64.17$ mV/dec., $S_{Ca}^{2+} = 38.33$ mV/dec., and $S_{pH} = -46.33$ mV/dec.) and selectivity for the detection of desired ions. The sensor suite was tested for on-body during running exercise for over 60 min; results show an increasing trend in $K^+$ and pH levels and decreasing trend of $Ca^{2+}$ levels in real sweat, as expected. The developed device can be a pivotal tool for point-of-care applications for in-field sweat ionic content and pH analysis.

Index Terms—Chemical and biological sensors, calcium sensor, flexible electronics, ion selective electrode, Internet of Things (IoT), multiplexed sensor, pH sensor, potassium sensor, sweat.

## I. INTRODUCTION

Wearable biosensor development has accelerated in recent years due to its potential to improve one's health and wellness without the need for specialized equipment or personnel [1], [2], [3]. Despite the advancement of several cutting-edge sensor technologies, commercially viable biosensors are predominantly limited to physical activity or biopotential monitoring due to the ease of integrating with electronics. On the contrary, biosensor integration with electronics has been challenging [4]. This is primarily because in most cases, the collection of human bodily fluids, such as blood, serum, and interstitial fluids (ISF) requires invasive approaches, which makes real-time analysis of biomarkers in these fluids, using said biosensors, not only more difficult but also poses a risk of infection at the collection site. However, collecting bodily fluids, such as sweat and saliva from human subjects is relatively easy, noninvasive, and most importantly, they contain several electrolytes and metabolites that are major biomarkers of mental and physical health conditions and correlated strongly with levels in blood [5]. To be more specific, sweat's sodium ($Na^+$), potassium ($K^+$), and pH can provide insight into the individuals' hydration state, which can further be utilized to detect fatigue or disorders related to electrolyte imbalance [7]. Similarly, improper calcium ion ($Ca^{2+}$) levels in sweat can endanger the correct functioning of numerous organs and systems, including but not limited to myeloma, cirrhosis, and normocalcemic hyperparathyroidism [8], [9], [10]. Thus, real-time monitoring of the pH and ionic content of sweat can be used to both detect various medical disorders in patients and to improve athletes' performance during competitions [11].

For a healthy person, the sweat pH changes from 4.5 to 6.5 [12], [13]. There is an increase in sweat pH with physical activity [13]. Similarly, the concentration of sweat calcium varies from 0.5 to 2.0 mM [14], [15], [16], while the concentration of sweat potassium ranges from 3.0 to 10.0 mM [17].

Corresponding author: Sameer Sonkusale (e-mail: sameer@ece.tufts.edu).
Associate Editor: J. B. Lee.
Digital Object Identifier 10.1109/LSENS.2023.3300827

Our research focus is on the development of sweat biosensors based on an electrochemical approach, specifically using potentiometry, due to its simplicity and compact wearable realization. There have been several examples of wearable biosensors, such as battery-less multiplexed pH, lactate, glucose, and chloride sensors [11], as well as $H^+$, $Na^+$, $K^+$, and $Cl^-$ sensors for sweat [18], [19], [20]. Also, recently an interesting approach based on the textile thread for sweat monitoring of $Na^+$, $NH_4^+$, pH, and lactate was reported [21]. However, very few configurations have been reported for the specific multiplexed detection of cationic contents ($K^+$ and $Ca^{2+}$ levels) in sweat with integrated Internet-of-Things (IoT) functionality. Addressing this research gap in the work, we illustrate the construction of a multiplexed sensor for these ionic species. The contributions of this work are 1) real-time detection of $K^+$, $Ca^{2+}$, and pH in a multiplexed sensor format with IoT integration, and 2) improved low-cost roll-to-roll sensor fabrication in flexible polyimide substrate.

## II. SENSOR FABRICATION

### A. Screen-Printed Electrode Fabrication

The proposed sensor has three planer working electrodes (WE) and one common reference electrode (RE). The three working electrodes are dedicated to potassium ($WE_K^+$), calcium ($WE_{Ca}^{2+}$), and pH ($WE_{pH}$) detection. The size of the whole sensor patch is 4 × 4 cm, while the diameter of the working and the reference electrode is 2 mm. First, the transfer tape (Chartpak, DAF8) is kept inside of the $CO_2$ laser (BOSS Model No: LS1416). Next, the origin is selected, the laser is focused, and framed to begin laser cutting. Finally, the transfer tape is cut according to the designed pattern. Then, the individual sensor pattern is separated from the main roll using a pair of scissors. Thereafter, the patterned transfer tape is attached to the polyimide sheet (thickness 0.002").

The next step is the traditional screen-printing stage. To fabricate a reference electrode made of silver/silver chloride (Ag/AgCl), the Ag/AgCl paste (Kayakli, AG-500A) is applied on one of the electrodes.

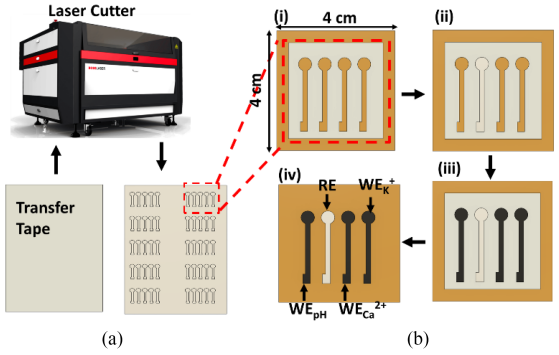


Fig. 1. (a) Stencil is cut on a transfer tape using a laser cutter. (b) (i) Polyimide with screen mask is screen printed with (ii) Ag/AgCl ink for RE, and (iii) carbon ink for WE followed by functionalization or drop casting of (iv) functional inks to realize sensors. Diameter of electrodes is 2 mm.

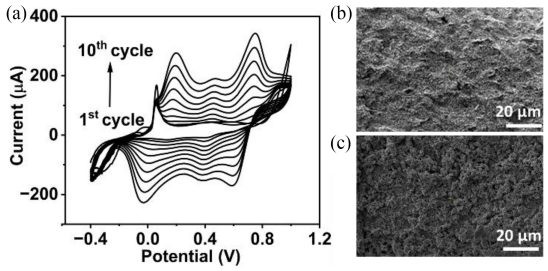


Fig. 2. (a) PANI deposition in 0.50-M aniline and 1.0 M of HCl using cyclic voltammetry by sweeping the voltage from −0.40 to 1.0 V at 50.0 mV/s. SEM image of (b) carbon-coated WE and (c) PANI-coated WE.

The paste was uniformly spread using a squeegee and the electrode was baked on a hot plate at 60 °C for 30 min. Thereafter, carbon ink (Kayakli, C-250J) is applied on to the other three electrodes to fabricate WE's and baked again at 65 °C for 30 min. Finally, the transfer tape is removed, and the bare electrodes are prepared. Fig. 1 shows the overall process of the fabrication process of the electrodes.

### B. Synthesis of $K^+$ and $Ca^{2+}$ ISM Coating

To prepare the $K^+$ ion-selective membrane (ISM) cocktail, 2.0% potassium ionophore I (valinomycin), 0.6% Sodium tetrakis[35-bis(trifluoromethyl) phenyl] borate, 64.7% bis(2-ethylhexyl) sebacate (DOS), and 32.7% polyvinyl chloride (PVC; high molecular weight) (w/w%) is dissolved in 1.0 mL of THF followed by 10 min of vortex shaking and 15 min of sonication.

The calcium ISM is made on 660 $\mu$L of THF, where 1.0% calcium ionophore, 65.45% DOS, 0.5% Sodium tetrakis[35-bis (trifluoromethyl)phenyl]borate, and 33.0% PVC is dissolved. The resulting cocktail is centrifuged at 750 r/min for 3 h to make a uniform cocktail.

### C. pH Sensitive Coating Synthesis

Our previous reports have detailed the procedure of formation of polyaniline (PANI)-based nanofiber coated $WE_{pH}$. Briefly, 1.0 M of HCl with 0.50 M of aniline is applied over the $WE_{pH}$, $WE_K^+$, and RE. PANI was potentiometrically deposited by sweeping voltage −0.4 to 1.0 V at 50.0 mV/s [Fig. 2(a)] and further grown at a fixed potential of 0.80 V for 600 s to facilitate the fabrication of uniform PANI nanofiber [22]. Then, the electrode was washed thoroughly to remove

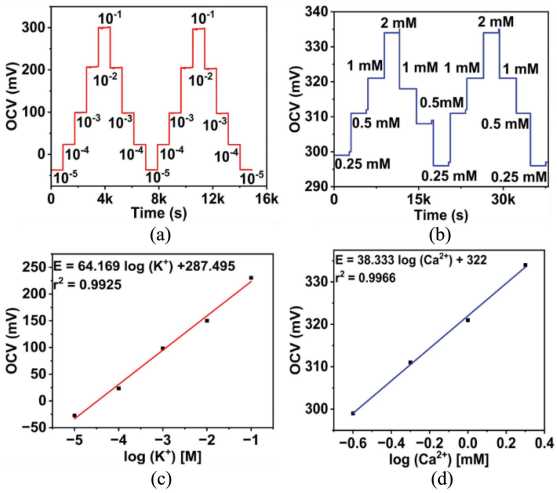


Fig. 3. Open-circuit voltage (OCV) responses for different concentrations of (a) potassium ion and (b) calcium ion. The calibration curve shows (c) OCV versus $K^+$ concentrations and (d) OCV versus $Ca^{2+}$ concentrations.

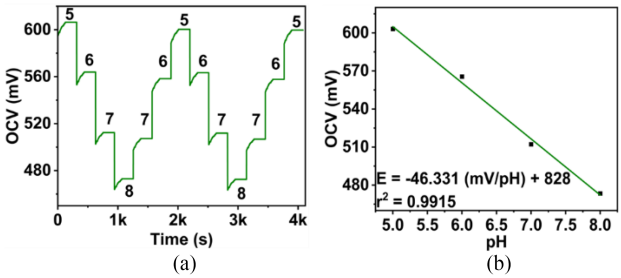


Fig. 4. (a) Open-circuit voltage (OCV) responses for different pH and (b) calibration curve for pH sensor: OCV versus pH.

the unbound monomers and acid impurities. Furthermore, the surface modification was characterized using scanning electron microscopy (SEM). Fig. 2(b) and (c) confirm that the electrode surface is fully covered after PANI deposition.

### D. Electrode Fabrication

5.0 $\mu$L of PEDOT: PSS (1.3wt% in water) is applied over the $WE_{Ca}^{2+}$ and dried overnight. Similar to the pH coating PANI layer is deposited over a working electrode to fabricate a cation exchange membrane for the potassium sensor ($WE_K^+$) and also kept at room temperature overnight.

Finally, 5.0 $\mu$L of K-ISM and Ca-ISM is applied over $WE_K^+$ and $WE_{Ca}^{2+}$, respectively. The electrodes were kept in the dark overnight at 25 °C for further use. The real-time data on the body is taken by separating the electrodes by using a clinical gauge.

## III. RESULTS AND DISCUSSION

### A. Potentiometric Detection of $K^+$, $Ca^{2+}$, and pH

All the calibration is done in artificial sweat which was prepared using the protocol described in the previous report [23]. The $K^+$ is calibrated for the range $10^{-1}$–$10^{-5}$ M (Fig. 3). Similarly, the $Ca^{2+}$ sensor is calibrated for the 0.25–2.0 mM range (Fig. 3), and the pH sensor is calibrated from pH 5.0–pH 8.0 range (Fig. 4). The sensors show

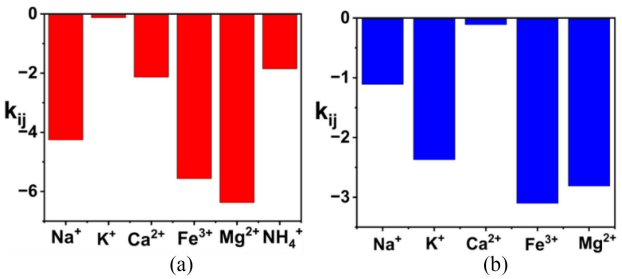


Fig. 5. Selectivity coefficient of (a) $K^+$; (b) $Ca^{2+}$ in the presence of various interfering species.

both repeatability and dynamic behavior for both low-to-high concentrations, and high-to-low concentrations. The monovalent cation ($K^+$) as well as the pH sensor shows near Nernstian behavior while due to the divacancy of $Ca^{2+}$, sensitivity to $Ca^{2+}$ is less than the expected Nernstian limit [24]. The coefficient of variance from cycle to cycle is less than 0.381%.

## B. Selectivity Test

The selectivity coefficient is calculated using the Nernst equation [25]

$$E = E^0 + \frac{RT}{z_i F} \ln\left[ a_i + \sum K_{ij}^{POT} a_j^{\frac{z_i}{z_j}} \right]$$

where $E$, $E^0$, $R$, $T$, $z$, and $F$ are denoted by electrode potential, standard electrode potential, gas constant, absolute temperature, valance of the ion, and Faraday constant, respectively. In addition, $a$ is the activity of the ion, and $i$ and $j$ represent the target and interfering ion, respectively. In all cases, 0.1 M of cations are chosen for the selectivity testing. While PANI improves the selectivity of the $K^+$ ions [26], [27] by working as a cation exchange membrane, PEDOT: PSS similarly improves the selectivity for $Ca^{2+}$. The overall selectivity results are shown in Fig. 5. According to the abovementioned equation, the coefficient $k_{ij}$ is the measure of the selectivity of the sensor. In the case of the interfering ions, the value of the $k_{ij}$ will be higher and in the case of the ion of interest it will be lower. In our case, the working electrodes are modified for selective detection of $K^+$ and $Ca^{2+}$. As shown in Fig. 5, the value of $k_{ij}$ for $K^+$ and $Ca^{2+}$ is lower, and the value of $k_{ij}$ of the interfering ions ($Na^+$, $Fe^{3+}$, $Mg^{2+}$, and $NH_4^+$) is higher. The reported $k_{ij}$ levels in Fig. 5 are adequate to conclude the said sensors for $K^+$ and $Ca^{2+}$ ions are selective and have less sensitivity to interfering ions.

## C. System Architecture and Real-Time Measurement

Arduino nano 33 microcontrollers operating at 3.3 V is used as an IoT interface to measure the sensor's open-circuit potential (OCP) with a built-in ADC (10 bit). It then calculates the concentration and pH levels and finally sends the data to the Blynk cloud platform from where the data are displayed on the user's smartphone. To monitor the ionic content and pH in sweat in the field, an additional OLED display has been added, while the Android Blynk app user interface is modified to monitor the data remotely. The OLED communicates with the microcontroller through $I^2C$ communication while the data are transmitted from the Arduino nano 33 IoT using Wi-Fi to the virtual port of the Blynk platform. The microcontroller-measured data and the commercial potentiostat (CHI 760)-measured data have a 0.0366% coefficient of variance. The system consumes almost 88.58 mW of power and has a latency (the time difference between data acquisition to the data update on the smartphone screen) of almost 3.05 s, which can be decreased with increased data rate (i.e., increased power consumption). The detailed system architecture and the real-time data acquisition are shown in Fig. 6.

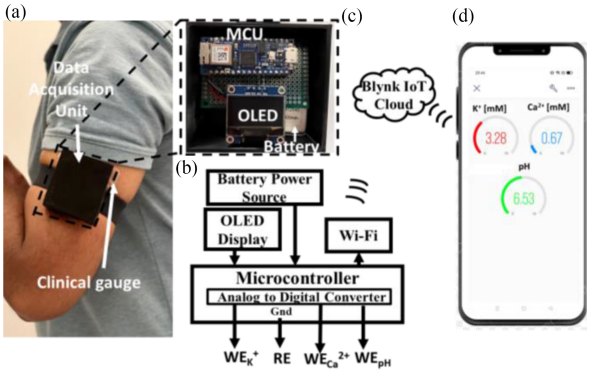


Fig. 6. (a) Sensor patch on hand with data acquisition unit. (b) System architecture. (c) Data to the blynk cloud. (d) Developed IoT app for real-time monitoring of the sweat ionic content and pH.

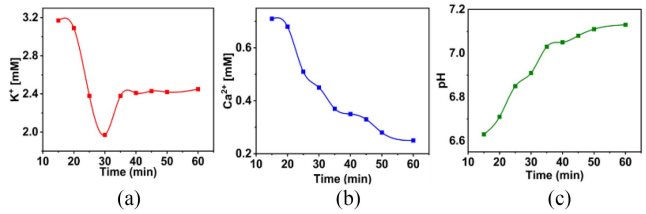


Fig. 7. Real-time on-body measurement of the sweat. (a) Potassium, (b) calcium, and (c) pH for a period of 1 h.

The system is also tested for on-body measurement in a single human volunteer under informed consent in a preapproved protocol. The sensor was affixed on the arm having a gauge underneath to continuously sample the sweat and data are acquired through the developed system described earlier. To perform on-body test, continuous running (856.35 calories burnt in total) for 1 h at 22 °C and 55%RH environment is performed. The first 15-min data were not considered as the body needs time to sweat. After the initial rise, the $K^+$ and $Ca^{2+}$ concentration in the sweat decreased during physical exercise. Similarly, the pH of the sweat becomes less acidic as the time of exercise increases. This phenomenon (Fig. 7) is in good agreement with existing literature [18], [28].

# IV. CONCLUSION

In this letter, we demonstrate accurate measurement of two cationic elements ($K^+$ and $Ca^{2+}$) and pH in the sweat using a multiplexed flexible sensor coupled with an embedded IoT platform. The sensor platform was validated using artificial sweat on the body during an exercise. However, more real-time on-body data needs to be collected to further validate the sensor performance and to correlate sweat ionic patterns to optimal athletes' performance in sports, and to several medical conditions to prevent life-threatening events. In the future, systems will be developed for multiplexed detection of several other sweat biomarkers (cortisol, uric acid, lactate, glucose, tyrosine, etc.) along with other ionic elements using advances in flexible electronics and electroanalytical chemistry.

## ACKNOWLEDGMENT

This work was supported in part by the NSF under Grant 1935555 and in part by the DoD CDMRP under Grant W81XWH-20-1-0589.

This work involved human subjects or animals in its research. Approval of all ethical and experimental procedures and protocols was granted by Human subject study is supported under the protocol approved for Center for Applied Brain and Cognitive Sciences (CABCS) at Tufts University.

## REFERENCES

[1] M. C. Brothers et al., "Achievements and challenges for real-time sensing of analytes in sweat within wearable platforms," *Accounts Chem. Res.*, vol. 52, pp. 297–306, 2019.

[2] A. J. Bandodkar, W. J. Jeang, R. Ghaffari, and J. A. Rogers, "Wearable sensors for biochemical sweat analysis," *Annu. Rev. Anal. Chem.*, vol. 12, pp. 1–22, 2019.

[3] M. McCaul, T. Glennon, and D. Diamond, "Challenges and opportunities in wearable technology for biochemical analysis in sweat," *Curr. Opin. Electrochemistry*, vol. 3, pp. 46–50, 2017.

[4] J. Heikenfeld et al., "Wearable sensors: Modalities, challenges, and prospects," *Lab Chip*, vol. 18, pp. 217–248, 2018.

[5] A. J. Bandodkar and J. Wang, "Non-invasive wearable electrochemical sensors: A review," *Trends Biotechnol.*, vol. 32, pp. 363–371, 2014.

[6] E. Scurati-Manzoni et al., "Electrolyte abnormalities in cystic fibrosis: Systematic review of the literature," *Pediatr. Nephrol.*, vol. 29, pp. 1015–1023, 2014.

[7] S. N. Cheuvront, R. Carter, and M. N. Sawka, "Fluid balance and endurance exercise performance," *Curr. Sports Med. Reports*, vol. 2, pp. 202–208, 2003.

[8] V. Young and C. Garza, "Dietary reference intakes for calcium, phosphorus, magnesium, vitamin D and fluoride," in *Standing Committee on the Scientific Evaluation of Dietary Reference Intakes, Food and Nutritional Board, Institute of Medicine*, Washington, DC, USA: Nat. Academy Press, 1997.

[9] W. G. Robertson, R. W. Marshall, and G. N. Bowers, "Ionized calcium in body fluids," *Crit. Rev. Clin. Lab. Sci.*, vol. 15, no. 2, pp. 85–125, 1981.

[10] R. S. Relman, "Metabolic consequences of acid-base disorders," *Kidney Int.*, vol. 1, pp. 347–359, 1972.

[11] A. Koh et al., "A soft, wearable microfluidic device for the capture, storage, and colorimetric sensing of sweat," *Sci. Transl. Med.*, vol. 8, no. 366, pp. 366ra165–366ra165, 2016.

[12] Z. Sonner et al., "The microfluidics of the eccrine sweat gland, including biomarker partitioning, transport, and biosensing implications," *Biomicrofluidics*, vol. 9, no. 3, 2015, Art. no. 031301.

[13] W. Dang, L. Manjakkal, W. T. Navaraj, L. Lorenzelli, V. Vinciguerra, and R. Dahiya, "Stretchable wireless system for sweat pH monitoring," *Biosensors Bioelectronics*, vol. 107, pp. 192–202, 2018.

[14] L. B. Baker, J. R. Stofan, H. C. Lukaski, and C. A. Horswill, "Exercise-induced trace mineral element concentration in regional versus whole-body wash-down sweat," *Int. J. Sport Nutr. Exercise Metab.*, vol. 21, no. 3, pp. 233–239, 2011.

[15] S. Katz, M. H. Schöni, and M. A. Bridges, "The calcium hypothesis of cystic fibrosis," *Cell Calcium*, vol. 5, no. 5, pp. 421–440, 1984.

[16] T. Verde, R. J. Shephard, P. Corey, and R. Moore, "Sweat composition in exercise and in heat," *J. Appl. Physiol.*, vol. 53, no. 6, pp. 1540–1545, 1982.

[17] S. J. Montain, S. N. Cheuvront, and H. C. Lukaski, "Sweat mineral-element responses during 7 h of exercise-heat stress," *Int. J. Sport Nutr. Exercise Metab.*, vol. 17, no. 6, pp. 574–582, 2007.

[18] H. Y. Y. Nyein et al., "Regional and correlative sweat analysis using high-throughput microfluidic sensing patches toward decoding sweat," *Sci. Adv.*, vol. 5, no. 8, 2019, Art. no. eaaw9906.

[19] H. Y. Y. Nyein et al., "A wearable microfluidic sensing patch for dynamic sweat secretion analysis," *Amer. Chem. Soc. Sensors*, vol. 3, pp. 944–952, 2018.

[20] M. Parrilla, I. Ortiz-Gómez, R. Cánovas, A. Salinas-Castillo, M. Cuartero, and G. A. Crespo, "Wearable potentiometric ion patch for on-body electrolyte monitoring in sweat: Toward a validation strategy to ensure physiological relevance," *Anal. Chem.*, vol. 91, pp. 8644–8651, 2019.

[21] T. T.-Thakoor et al., "Thread-based multiplexed sensor patch for real-time sweat monitoring," *npj Flexible Electron.*, vol. 4, no. 18, 2020, Art. no. 18.

[22] C. Asci, R. Del-Rio-Ruiz, A. Sharma, and S. Sonkusale, "Ingestible pH sensing-capsule with thread-based electrochemical sensors," in *Proc. IEEE Sensors*, 2022, pp. 1–4.

[23] W. Gao et al., "Fully integrated wearable sensor arrays for multiplexed in situ perspiration analysis," *Nature*, vol. 529, pp. 509–529, 2016.

[24] A. Ansaldi and S. I. Epstein, "Calcium ion-selective electrode in which a membrane contacts graphite directly," *Anal. Chem.*, vol. 45, no. 3, pp. 595–596, 1973.

[25] E. Bakker, E. Pretsch, and P. Bühlmann, "Selectivity of potentiometric ion sensors," *Anal. Chem.*, vol. 72, no. 6, pp. 1127–1133, 2000.

[26] T. Glennon et al., "'SWEATCH': A wearable platform for harvesting and analysing sweat sodium content," *Electroanalysis*, vol. 28, pp. 1283–1289, 2016.

[27] T. N. T. Tran, S. Qiu, and H.-J. Chung, "Potassium ion selective electrode using polyaniline and matrix-supported ion-selective PVC membrane," *IEEE Sensors J.*, vol. 18, no. 22, pp. 9081–9087, Nov. 2018.

[28] H. Y. Y. Nyein et al., "A wearable electrochemical platform for noninvasive simultaneous monitoring of $Ca^{2+}$ and pH," *Amer. Chem. Soc. Nano*, vol. 10, no. 7, pp. 7216–7224, 2016.